

# The Internal m=1 Mode in Burning Plasma Experiments

S.C. Jardin<sup>1</sup>, J. Breslau<sup>1</sup>, G. Fu<sup>1</sup>, N. Gorelenkov<sup>1</sup>, C.E. Kessel<sup>1</sup>, J. Manickam<sup>1</sup>, D. Meade<sup>1</sup>,  
W. Park<sup>1</sup>, H. Reimerdes<sup>2</sup>, H. Strauss<sup>3</sup>

<sup>1</sup>*Princeton Plasma Physics Laboratory, Princeton NJ 08540 USA*

<sup>2</sup>*Columbia University, New York, NY*

<sup>3</sup>*Courant Institute of Mathematical Science, New York University, New York, NY*

## abstract

We provide a summary of the Porcelli sawtooth model and compare the ideal term in that formulation with recent evaluations. The implementation in TSC is described. We give results for the application of this model, in combination with several leading transport models, as part of an integrated simulation of the three proposed burning plasma experiments: FIRE, ITER, and Ignitor. Both complete and partial reconnection is considered.

### Introduction:

One of the major uncertainties in the physics design of a burning plasma experiment is the behavior of the internal m=1 mode. The toroidal current in an inductively driven tokamak with low enough edge safety factor ( $q_s$ ) will normally continue to peak until a relaxation oscillation occurs, the so-called sawtooth crash. This flattens the central temperature and density, and redistributes the current and poloidal flux to some extent. The crash results in an outward transport of energy that will affect the fusion burn to some degree. The sawtooth crash could also couple to other plasma modes, for example the tearing modes and the edge localized modes, and it can interact with the energetic alpha particles to cause particle loss. We have undertaken an evaluation of the effects of the sawtooth in three candidate burning plasma experiments, ITER, FIRE, and Ignitor.

### The Porcelli Model:

A comprehensive model of the sawtooth trigger and relaxation oscillation has been developed by Porcelli *et al* [1]. We adopt the notation used in that paper. The macroscopic drive has with it associated an effective potential energy functional defined by:

$$dW = dW_{core} + dW_{fast}$$

where  $dW_{core} = dW_{MHD} + dW_{KO}$ . The potential energy is normalized according to

$$d\hat{W} \equiv -\frac{4dW}{s_1 \mathbf{x}^2 \mathbf{e}_1^2 RB^2},$$

with  $s$  being the magnetic shear,  $\mathbf{x}$  the radial displacement of the magnetic axis and  $\mathbf{e}$  the inverse aspect ratio. The subscript 1 denotes values at the  $q=1$  surface. We drop the hat notation in the following discussion.

The ideal MHD potential energy term,  $dW_{MHD}$ , includes the effects of toroidicity and of plasma shaping in a free boundary plasma [2,3]. Since the Porcelli form for this term has been the subject of considerable debate and controversy, we discuss it and the justification for it here. We first note that it has now been demonstrated that the analytical [2,3] and numerical [3,4,5], evaluation of this term depends sensitively on the plasma boundary condition, and that calculations that assume a perfectly conducting wall on the surface of the plasma will give a misleadingly stable result [7-11].

### The Ideal Term:

We consider the Porcelli approximation to the ideal term [1]:

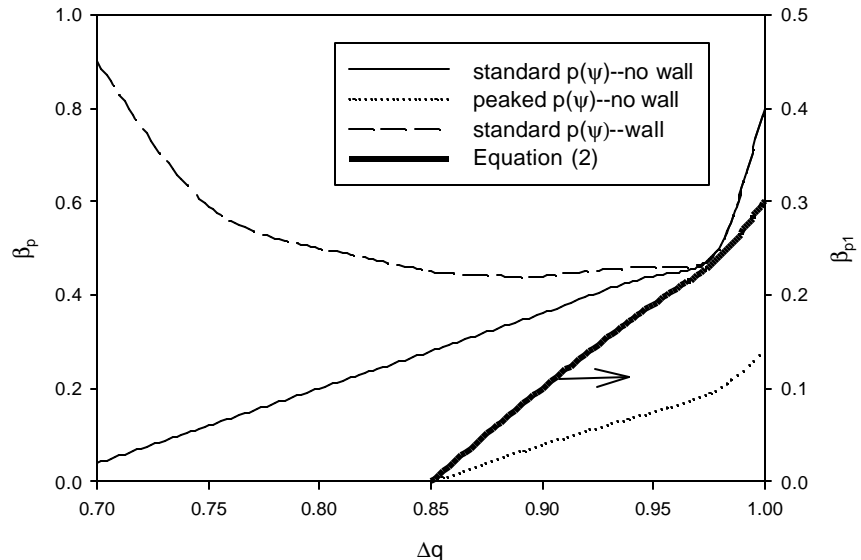
$$dW_{MHD} = -\frac{3p}{2} e_1^2 (b_{p1}^2 - b_{pc}^2) - \frac{p}{3} (\Delta q)^2 \left( \frac{k_1 - 1}{2} \right)^2 \quad (i)$$

Here,  $b_{p1} = (8p/B_{p1}^2) [\langle p \rangle_1 - p(r_1)]$ , with the brackets denoting volume averaging within the q=1 surface,  $b_{pc} = 0.3(1 - 5r_1/3a)$ ,  $\Delta q = 1 - q_0$ , and  $k_1$  is the plasma ellipticity at the q=1 surface. The first term in brackets in Eq. (i) is the Bussac result for parabolic profiles modified by removing the stabilizing effect of the wall. This reflects the fact that for circular cross section plasmas without a wall on the surface, the marginal  $b_p$  decreases monotonically with increasing q=1 radius [3].

The second term in Eq. (i) reflects the destabilizing effect of cross section shaping, and in particular how this effect decreases the critical  $b_{p1}$  as  $q_0$  decreases from 1. To see this, we solve Eq. (i) for the critical  $b_{p1}$  vs  $r_1/a$  for typical profiles with  $k_1 \sim 1.4$ ,  $\epsilon \sim 0.275$ , and a near parabolic q-profile with  $q_{edge} > 3$  so that  $Dq \sim 2.5 (r_1/a)^2$ . Solving Eq. (i) for  $dW=0$  yields:

$$eb_{p1} = \left[ (0.3e)^2 (1 - 5r_1/3a)^2 - \frac{r_1^2}{18a^2} \right]^{1/2} \quad (ii)$$

**Figure 1: Critical  $b_p$  vs  $Dq$  for Eq. (ii) and for several numerical equilibrium from PEST with differing pressure profiles and both with and without a conducting wall at the boundary of the plasma. Beta values above the curves are unstable to ideal modes.**



We plot the critical  $\mathbf{b}_{p1}$  vs  $\mathbf{D}q$  from Eq. (ii) and compare the result with recent numerical calculations [4] of  $\mathbf{b}_p$  vs  $\mathbf{D}q$  using PEST with the correct free-boundary conditions. For the purpose of displaying these results together, we note that for the profiles of interest, we have  $\mathbf{b}_p \sim 2 \mathbf{b}_{p1}$ . Eq. (ii) is seen to be qualitatively correct for a plasma without a wall, although the exact results are profile dependent.

### The Kinetic Terms:

The Porcelli model also includes the stabilizing effect of thermal trapped ions,  $dW_{KO}$  [12,13], and kinetic effects related to high energy particles (fusion alphas, ICRF accelerated ions and beam ions),  $dW_{fast}$  [14,15]. We have compared the latter term from [1] with a more exact calculation using NOVA-K and a computed alpha-particle slowing down distribution function from TRANSP. We find that the simplified expression in [1] agrees qualitatively with the more exact result from NOVA-K, and also quantitatively within a factor of  $\sqrt{2}$ . This is consistent with other comparisons of this term [15,16].

### The Trigger:

The Porcelli sawtooth model invokes an event if one of the following 3 criteria are met. The first is the condition that for the trapped-ion processional drift orbits to be effective in stabilizing the internal kink mode, the high-energy trapped particles must complete many orbits within a characteristic magnetic perturbation time. This condition is violated when

$$-d\widehat{W}_{core} > w_{Dh} t_A \quad (1)$$

The second condition is that the diamagnetic rotation be sufficient to stabilize the mode. Thus, the sawtooth will be triggered when

$$-d\widehat{W} > 0.5 w_{*i} t_A \quad (2)$$

If the energy drive is sufficiently weak that the mode is stable according to these 2 criteria, the  $m=1$  mode structure changes its nature from a global internal kink to a drift-tearing mode localized near the  $q=1$  surface. This is normally stable because of kinetic layer effects, but the layer effects will be insufficient when the normalized potential energy exceeds the normalized ion Larmor radius and rotation effects are sufficiently weak, i.e. when

$$\widehat{r} < -d\widehat{W} < 0.5 w_{*i} t_A \quad \text{and} \quad w_{*i} < \mathbf{g}_r \quad (3)$$

where  $\mathbf{g}_r$  is the characteristic growth rate of the internal kink mode in the ion-kinetic regime. The second inequality in (3) can also be translated into a condition that the magnetic shear at the  $q=1$  surface exceed a critical value for instability [1].

### The Sawtooth Crash:

When the sawtooth is predicted to be triggered by one or more of these 3 criteria, we modify the transport coefficients in two ways. The value of the toroidal flux at the inversion surface,  $\Phi_1$ , is calculated as

$$\int_0^{\Phi_1} \left( \frac{1}{q(\Phi)} - 1 \right) d\Phi = 0$$

For the duration of the sawtooth crash time  $\tau_{\text{CRASH}}$ , we define the thermal conductivity and the hyper-resistivity to be:  $\chi = \Gamma_1^2 / \tau_{\text{CRASH}}$  and  $\lambda = \lambda_0 B_0^2 \Gamma_1^4 / \tau_{\text{CRASH}}$ . A value of  $\lambda_0 = 0.1$  effectively causes a Kadomtsev reconnection to occur [17] in the time  $t = \tau_{\text{CRASH}}$ , which we took to be 10 ms in these runs. By lowering  $\lambda_0$  to 0.001, we can model an incomplete reconnection where the temperature profile flattens but the current and flux do not fully reconnect.

### **Integrated Modeling:**

It has previously been reported that the Porcelli sawtooth model described here has been implemented in the PRETOR code and compared in detail with JET experiments in several different regimes with different levels of NBI power. It was reported that in every case analyzed, the simulated sawtooth periods are within 20% of the experimentally observed periods, even as the period varies by more than a factor of 5 during a given shot [18]. We have implemented this same Porcelli sawtooth model in the Tokamak Simulation Code (TSC)[19] and have investigated its consequences on transport and ignition in the three proposed burning plasma experiments.

### **Core Transport and Boundary Conditions:**

There are several transport models that have been developed for use in predicting the profiles and performance in a burning plasma. We have implemented three of the leading models in TSC. The three models are (A) the Multi-mode model [20], (B) the Gyro-Landau Fluid model GLF23 [21], and (C) the ‘‘standard TSC’’ Coppi-Tang model [19]. These core transport models must be supplemented by boundary and edge models.

The H-mode models (A) and (B) are only applied in the central region  $0 < \Phi < 0.75$ , where  $\Phi$  is the normalized toroidal magnetic flux that is zero at the magnetic axis and unity at the plasma/vacuum separatrix. In the edge region  $0.75 < \Phi < 1.0$ , we use a transport model  $\chi_i = \chi_e = C/n_e$ , where  $n_e$  is the local electron density and C is a constant chosen so as to make the pressure gradient in this region below the infinite-n ballooning mode stability criteria. This leads to electron and ion temperatures at the top of the pedestal,  $\Phi = 0.75$ , of 3-5 KeV.

The density profile is not advanced in time in these simulations, but is rather a prescribed function of normalized poloidal flux,  $\psi$ , and time,  $t$ . We take the electron density during the current flattop to be  $n_e(\psi, t) = n_0(t) \times [(1 - \psi^\beta)^\alpha + r_{\text{edge}}]$ , with  $\alpha=0.3$ ,  $\beta=2.25$ ,  $n_0 = 4.0 \times 10^{20}$  and  $r_{\text{edge}} = 0.3$  for FIRE, with  $\alpha=0.25$ ,  $\beta=8.0$ ,  $n_0 = 0.75 \times 10^{20}$  and  $r_{\text{edge}} = 0.4$  for ITER, and with  $\alpha=1.2$ ,  $\beta=1.2$ ,  $n_0 = 9.0 \times 10^{20}$  and  $r_{\text{edge}} = 0.1$  for Ignitor.

### **Discharge Simulations of FIRE:**

We have developed a full 1 1/2D TSC simulation of a complete FIRE discharge including current rampup, flattop, burn, and current rampdown for each of the three transport models, and utilizing the Porcelli sawtooth model with both complete and incomplete reconnection.

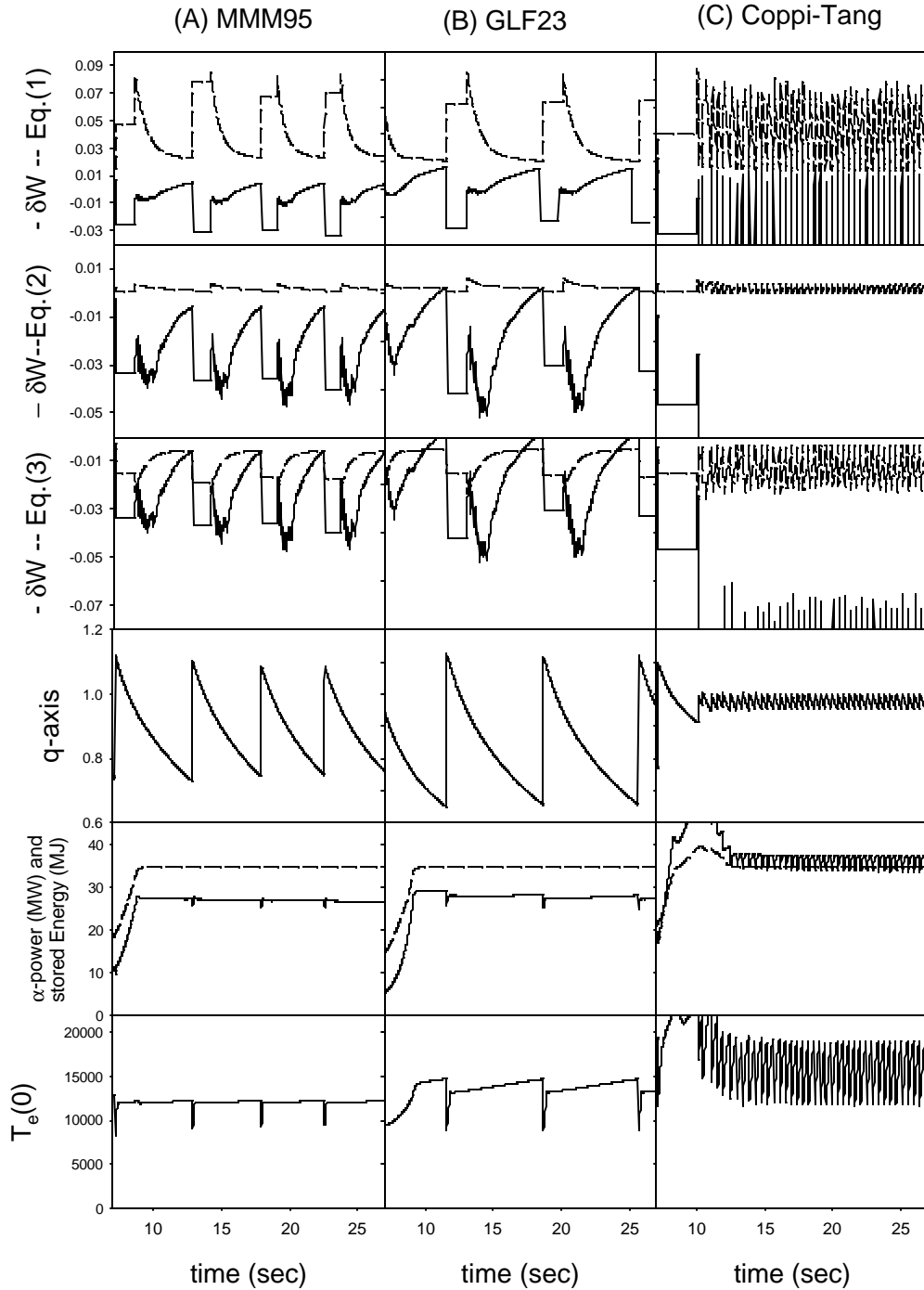


**Figure 2: The complete reconnection Porcelli model. The top three frames show  $dW$  (solid) and the critical value (dashed) for the 3 transport models for the 3 criteria corresponding to Eqns. (1)-(3). During the flattop, for the simulation using model (A), the sawtooth is triggered by criteria 3, for model (B) it is criteria 2, and for model (C) it is criteria 1. The 4<sup>th</sup> row shows the safety factor on axis for each of the 3 models. The next row shows the total stored energy (W) (dashed line) and the instantaneous  $\alpha$ -power (solid line), and the final row the central electron temperature.**

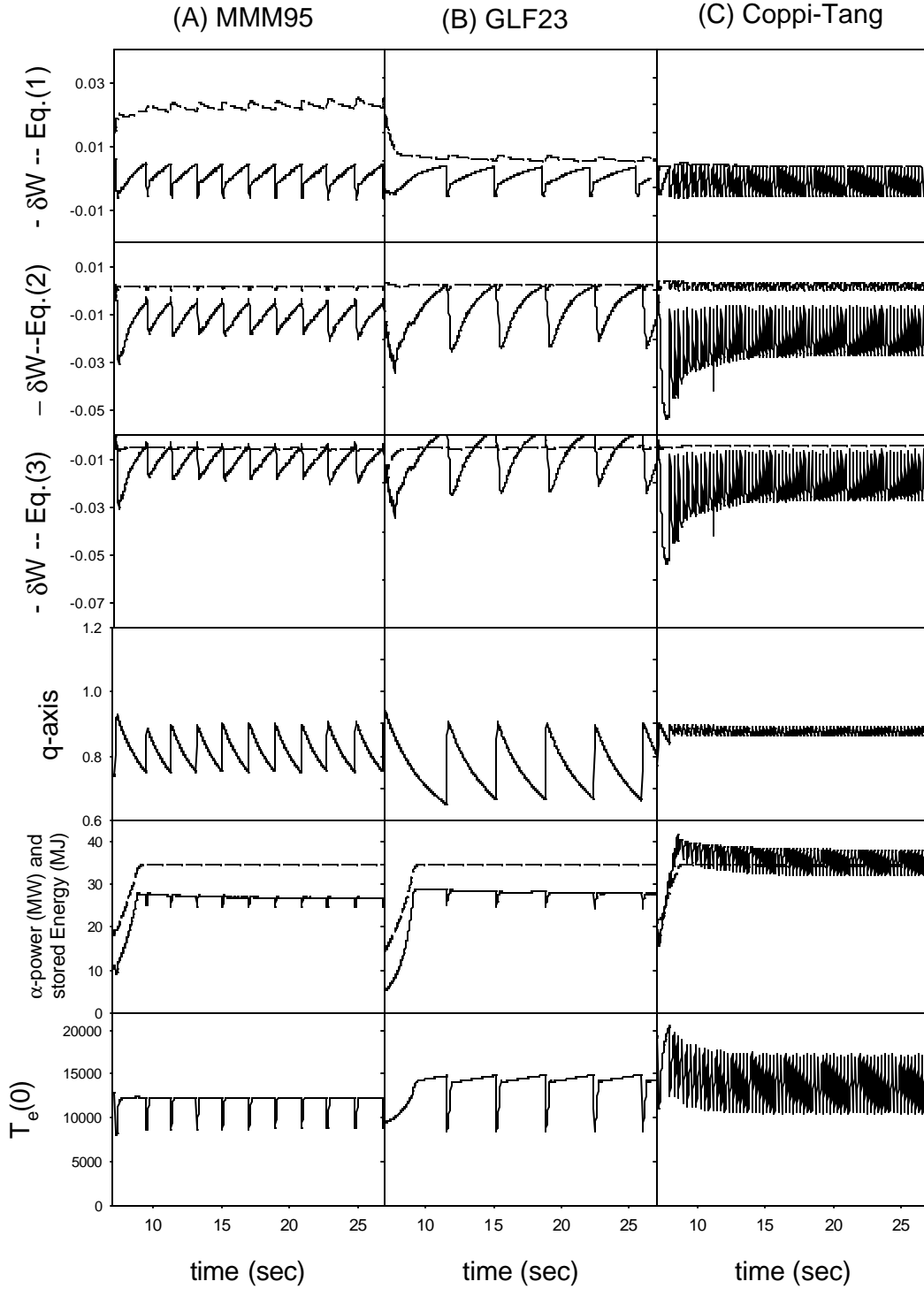
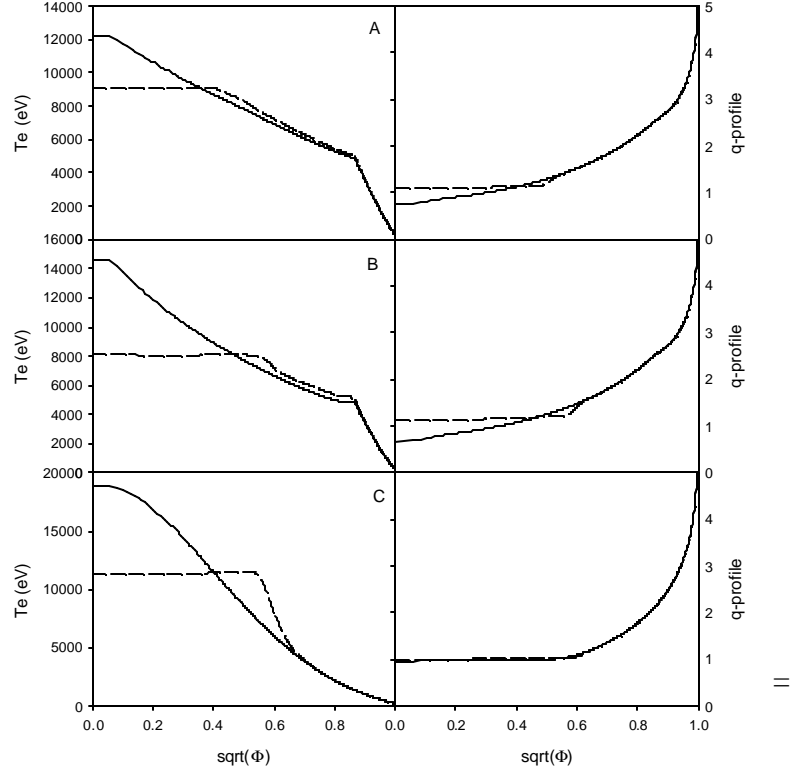


**Figure 3: Three FIRE simulations with the three different transport models (same as Figure 2) but for an incomplete reconnection model. The time averaged results are very similar, but the sawtooth period is reduced by about a factor of 2.**

**Figure 4: Electron temperature and safety-factor profiles just before (solid) and after (dotted) a sawtooth crash for the (A) MMM95, (B) GLF23, and (C) Coppi-Tang transport simulations corresponding to the complete reconnection simulations of Figure 2.**

We utilize a feedback system on the ICRH power designed to keep the total stored energy  $W$  constant at 34.5 MJ of total stored energy. We also include a uniform distribution of 3% Beryllium impurity, which together with the He buildup (assuming  $\tau_P$  5 sec), leads to a value of  $Z_{EFF} \sim 1.4$  during the flattop. The constant in the edge region is chosen as  $C=2 \cdot 10^{19}$  for H-mode models (A) and (B). For transport model (C), we choose coefficients  $(a_{121}, a_{122}) = (0.10, 0.42)$  and impose a separatrix temperature at  $\Phi = 1.00$  of  $T_e = T_i = 400$  eV.



The results of these simulations are presented in Figures 2-4. Figure 2 shows the results of using the complete reconnection Porcelli model together with each of the 3 transport model. Each of the 3 transport models leads to a different behavior of the sawtooth as shown in these figures. The model A (MMM95) has sawteeth every  $\sim 5$  seconds triggered by the criteria in Eq. (3), the model B (GLF23) has sawteeth every  $\sim 7$  seconds, triggered by the criteria in Eq. (2). In model C (Coppi-Tang), the sawteeth occur much more frequently, about every 0.5-second, and are triggered by the criteria in Eq. (1). We expect the H-mode models A and B to be more representative of what will happen in the actual experiment, but have included model C for contrast.

The electron temperature and safety factor profiles just before and after the last crash for these runs are shown in Figure 4. The instantaneous alpha power production and total stored energy stay relatively constant in each of these runs, as shown in the bottom row of Figure 2.

When these runs are repeated but using the incomplete reconnection model ( $\lambda_0=0.001$ ), we find very similar results (see Figure 3), with the primary difference being that the sawtooth frequency increases (2 sec, 3.5 sec, 0.2 sec) and the excursion in  $q$  is less [( $.75,.90$ ), ( $.67,.90$ ), ( $.86,.89$ )], but the performance, stored energy, alpha power, and Q value are essentially unchanged. This follows from the fact that the sawtooth period is long compared to the energy confinement time, and the plasma is at a sufficiently high temperature that even when the central temperature is redistributed, the central region of the plasma is still near the 10keV peak in the fusion power production cross section.

**Discharge Simulations of ITER:**

For the ITER simulations we use the Gyro-Landau Fluid model GLF23 [21], referred to above as model (B). We utilize a feedback system on the ICRH power designed to keep the total stored energy  $W$  constant at 320 MJ of total stored energy. We also include a uniform distribution of 2% Beryllium and 0.12% Argon impurities, which together with the He buildup (assuming  $\tau_P$

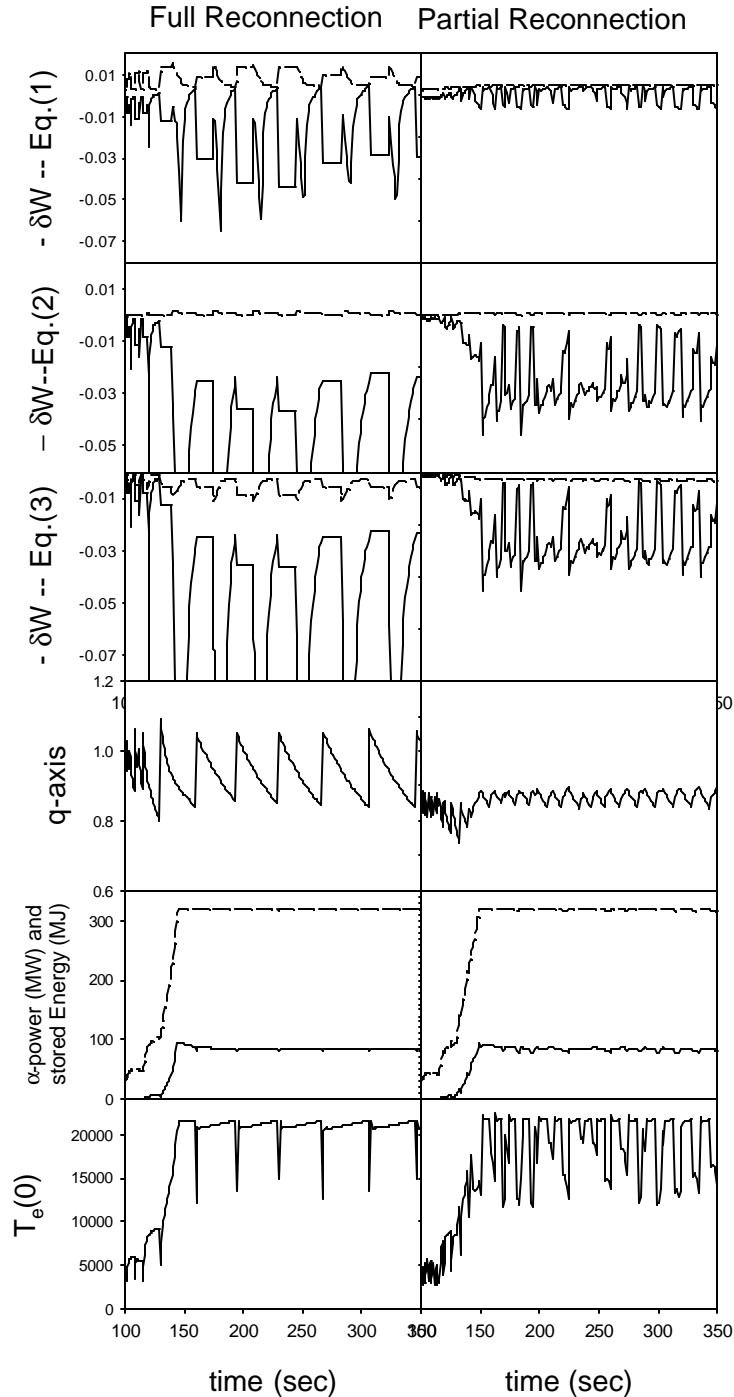


Figure 5: ITER simulations using the GLF23 transport model and both the complete and incomplete reconnection models.



= 18.5 sec), leads to a value of  $Z_{\text{EFF}} \sim 1.65$  during the flattop. The constant in the edge region is chosen as  $C=2.5 \times 10^{19}$ .

The results of two simulations are shown in figure 5, one using complete reconnection and the other with incomplete reconnection. The sawteeth are predominantly triggered by the criteria in Equation (1) for the ITER simulations. Note that the sawtooth period is about every 50 sec during the flattop for the complete reconnection, and 2-3 times that frequent for the incomplete reconnection. As in the FIRE simulations, both the alpha power and stored energy are essentially independent of the sawtooth period, since the period is always longer than the energy confinement time and the central temperature is so high.

### Discharge Simulations of Ignitor:

For the Ignitor model, we use the (Coppi-Tang) transport model with coefficients  $(a_{121}, a_{122}) = (0.035, 0.21)$  since it is limited and primarily ohmically heated. We assume a value of  $Z_{\text{EFF}} = 1.2$  in the radiation and the resistivity calculations without explicitly introducing an impurity. We apply 5 MW of external ICRH power. A separatrix temperature at  $\Phi = 1.00$  of  $T_e = T_i = 10$  eV is imposed.

We see that the sawtooth is triggered by the criteria in Equation (2) in these Ignitor simulations. The period is

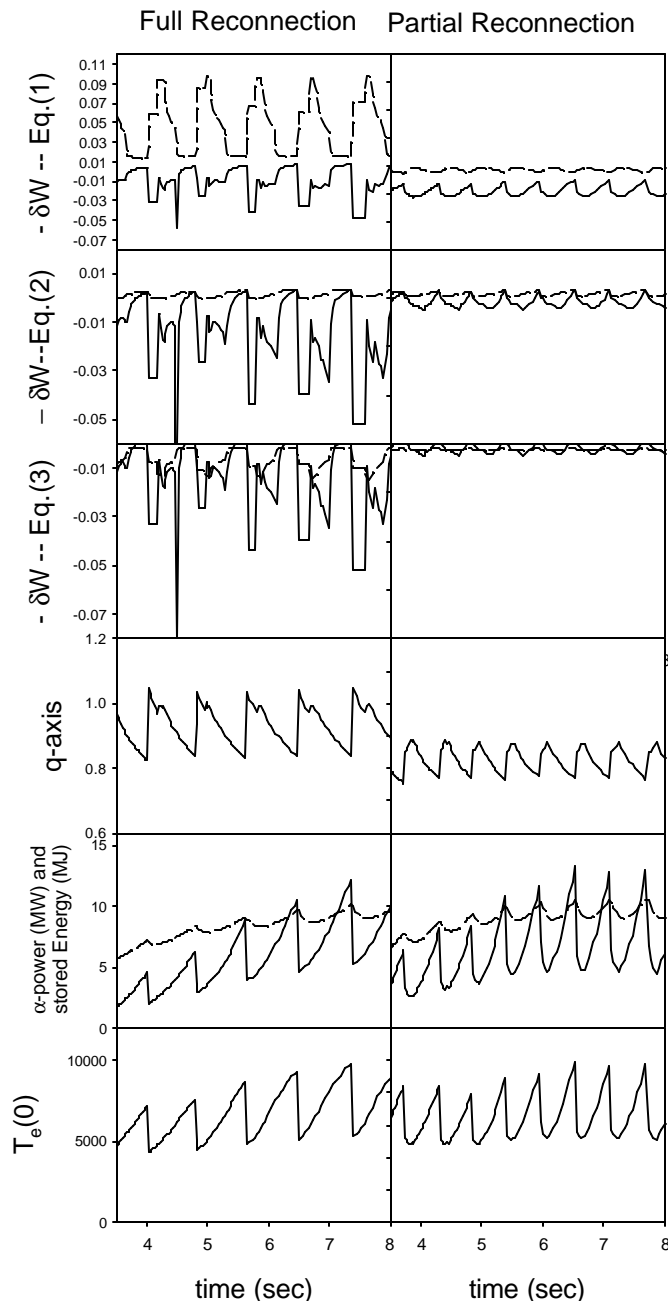


Figure 6: Ignitor simulation using the Coppi/Tang transport model and both the complete and incomplete reconnection Porcelli model

about 1 sec in the complete reconnection simulations and 600 ms in the incomplete reconnection simulation. The sawtooth does have a substantial effect on the neutron yield since it is comparable to the energy confinement time, and also because the central temperature is less than the temperature where the DT reaction rate takes on a maximum. Thus, the redistribution of the energy during the sawtooth crash results in a lowering of the instantaneous neutron production.

### **Future Work**

The nonlinear M3D code is also being used to investigate the assumptions made in the Porcelli model and to evaluate the consequences of the sawtooth crash in burning plasma devices, including the effects on the high-energy Helium population, the formation of stochastic regions outside the  $q=1$  surface, and the coupling of the  $m=1$  mode to other modes. Results of this study will be reported separately.

### **Summary and Conclusions:**

Each of the three burning plasma experiment under consideration is primarily inductively driven and is expected to exhibit sawtooth oscillations. Fast particle stabilization is an important effect, and leads to expansion of the  $q=1$  surface until the crash occurs. There is some uncertainty as to whether the crash will result in a complete Kadomtsev reconnection, or a partial reconnection, and so we have evaluated the effects of both.

We find that in both FIRE and in ITER, the sawtooth leads to periodic oscillations on a time that is considerably longer than the energy confinement time,  $\tau_{SAW} \gg \tau_E$ , and that the temperature at the  $q=1$  surface is sufficiently high that the sawteeth oscillations have negligible effect on both the stored energy and the rate of neutron production. The incomplete reconnection sawteeth have a period about half that of the complete reconnection, but still long compared to  $\tau_E$ .

In Ignitor, we find that the sawtooth period is comparable to the energy confinement time, and that the temperature at the  $q=1$  surface is sufficiently low that the neutron production rate will oscillate substantially along with the sawtooth oscillation. However, this is not considered to be a serious flaw in the device, and it may, in fact, be possible to operate in a regime with higher temperature and less frequent sawteeth so that this is not an issue.

We note that the results presented here are somewhat sensitive to the choice of the transport model chosen, and thus cannot be taken as definitive. However, the GLF23 and MMM95 do give similar results for the sawtooth behavior in the (H-mode) FIRE simulations, and the Coppi-Tang model has given good results when compared in detail with ohmic discharges in TFTR [19]. However, more calibration of these models in existing experiments is clearly needed.

### **Acknowledgements:**

The authors have benefited from discussions and cooperation from G. Bateman, J. Kinsey, and A. Kritz. The MMM95 and GLF23 subroutines were downloaded from the NTCC library. This work was supported by DOE Contract # DE-AC02-76CHO3073.

## REFERENCES

- [1] Porcelli F.; Boucher D; Rosenbluth M; *Plas. Phys. and Cont. Fusion* **38** (1996) 2163
- [2] Bussac MN, Pellat R, Edery D and Soule JL 1975 *Phys. Rev. Lett.* **35** 1638
- [3] Lutjens H, Bondeson A and Vlad G 1992 *Nucl. Fusion* **32** 1625
- [4] Manickam, private communication (2002)
- [5] Reimerdes H, Pochelon A, *et al*, *Plas. Phys. and Cont. Fusion* **42** (2000) 629
- [6] Manickam J, *Nucl. Fusion*, **24** (1984) 595
- [7] Coppi AC, Coppi B, *Nucl. Fusion* **32** (1992) 205
- [8] Detragiache P, *Plasma Phys. Cont. Fusion* **40** (1998) 1501
- [9] Wahlberg C, J. Plasma Phys. **62** (1999) 1621
- [10] Eriksson HG, Wahlberg C., *Phys. Plasmas*, **9**, (2002) 1606
- [11] Bombarda F, et al, *Nucl. Fusion* **38** (1998) 1861
- [12] Kuvshinov B N and Mikhailovskii A B 1987 *Sov J. Plasma Phys* **13** 527
- [13] Antonsen T M Jr and Bondeson A 1993 *Phys. Fluids B* **5** 4090
- [14] Coppi B, Migliuolo S, Pegoraro F and Porcelli F 1990 *Phys. Fluids B* **2** 927
- [15] Angioni C, Pochelon A, *et al*, *Plas. Phys. and Cont. Fusion* **44** (2002) 205
- [16] Graves JP, Gorelenkov NN, Sauter O, European Physical Society Meeting on Plasma Physics and Controlled Fusion, Montreux Switzerland, (2002)
- [17] Ward DJ and Jardin SC *Nucl Fusion* **29** (1989) 905
- [18] Angioni A, Pochelon A, et al, *Plas. Phys. and Cont. Fusion* **44** (2002) 205
- [19] Jardin SC; Bell MG; Pomphrey N; *Nucl Fusion* **33** (1993) 371
- [20] Bateman, G; Kritz AH; Kinsey JE; Redd AJ, *Physics of Plasmas* **5** (1998) 2355
- [21] Waltz R; et al, *Phys. Plasmas* **4** (1997) 1499